Original paper

Hydrogen bonding and structural complexity of the $Cu_3(AsO_4)(OH)_3$ polymorphs (clinoclase, gilmarite): a theoretical study

Sergey V. KRIVOVICHEV

Department of Crystallography, Institute of Earth Sciences, St. Petersburg State University, University Emb. 7/9, 199034 St. Petersburg, Russia; s.krivovichev@spbu.ru

Density functional theory (DFT) is used to determine positions of H atoms and to investigate hydrogen bonding in the crystal structures of two polymorphs of $Cu_3(AsO_4)(OH)_3$: clinoclase and gilmarite. Hydrogen bonds in clinoclase involve interactions between hydroxyl groups and O atoms of arsenate tetrahedra, whereas the crystal structure of gilmarite features OH···OH bonding, which is rather uncommon in copper hydroxy-oxysalts. Information-based parameters of structural complexity for clinoclase and gilmarite show that the former is more complex ($I_{G,total}$ = 213.212 bits/cell) than the latter ($I_{G,total}$ = 53.303 bits/cell), which indirectly points out that gilmarite is metastable. This suggestion is supported by the lower density of gilmarite (4.264 g/cm^3) compared to that of clinoclase (4.397 g/cm^3). The hypothesis of metastable character of gilmarite is in agreement with the Goldsmith's simplexity principle and the Ostwald–Volmer rule.

Keywords: hydrogen bonding, clinoclase, gilmarite, density functional theory, structural complexity, metastability
Received: 4 January, 2017; accepted: 3 March, 2017; handling editor: J. Plášil

1. Introduction

Copper arsenates are important secondary phases in oxidation zones of mineral deposits and volcanic fumaroles (Plášil et al. 2014a, b; Pekov et al. 2015a, b, 2016 Krivovichev et al. 2016a; Majzlan et al. 2017). Usually, they form rather diverse mineral associations that may include metastable as well as stable mineral species (e.g., euchroite is metastable relative to olivenite, yet both minerals have been found in the same association – Magalhães et al. 1988; Majzlan et al. 2017). Clinoclase and gilmarite are two polymorphs of $Cu_3(AsO_4)(OH)_3$ that are essentially different in their natural occurrences. Whereas clinoclase had been known since 1801 (Bournon 1801) and found at more than a hundred localities worldwide, gilmarite was first described by Sarp and Černý (1999) from Roua copper mines, Alpes Maritimes, France. The two minerals are remarkably different in their crystal structures (Ghose et al. 1965; Eby and Hawthorne 1990; Sarp and Černý 1999). Due to the higher abundance of clinoclase compared to gilmarite, it has been studied by a number of techniques, including vibrational spectroscopy (Frost et al. 2002; Martens et al. 2003) and magnetic susceptibility measurements (Lebernegg et al. 2013). Since no H atom positions have been determined in the original structural studies (Ghose et al. 1965; Eby and Hawthorne 1990; Sarp and Černý 1999), Lebernegg et al. (2013) used density functional theory (DFT) to establish the hydrogen bonding scheme in clinoclase and to investigate the influence of the hydrogen positions on the magnetic coupling. However, questions remain concerning the relative stabilities of clinoclase and gilmarite that would explain the difference in their abundance in nature.

Recently, we have developed an approach to quantitative evaluation of structural complexity of minerals by the Shannon information theory that allows determination of this important parameter in terms of information amount per atom and per unit cell (Krivovichev 2012, 2013). Using statistical arguments, Krivovichev (2016) demonstrated that structural information per atom provides a negative contribution to configurational entropy of crystals and therefore is a physically important parameter.

One of the interesting implications of quantitative measures of structural complexity is that it provides the possibility to evaluate Goldsmith's (1953) simplexity principle in numerical terms. This principle states that, under appropriate kinetically favored crystallization regime (such as crystallization from supersaturated solutions or supercooled melts), the crystalline phase that may form in the system is not the most stable one, but very frequently metastable with the structure simpler than that of the stable phase. This principle found many examples in geological systems (Goldsmith 1953; Morse and Casey 1988) and its general validity was confirmed by means of the information-based measures (Krivovichev 2013, 2015).

The note is in order that structural complexity (or simplexity in Goldsmith's terms) is not the only parameter governing formation of metastable phases, but other parameters such as the structure of precursors and prenucleation clusters and influence of other phases during heterogeneous nucleation should be taken into account as

Tab. 1 Crystallographic data and structural complexity parameters for clinoclase and gilmarite

Parameters	Clinoclase	Gilmarite
Symmetry	Monoclinic	Triclinic
Space group	$P2_1/c$	$P1$
a [Å]	7.257	5.445
b [Å]	6.457	5.873
c [Å]	12.378	5.104
α [°]	90	114.950
β [°]	99.51	93.050
γ [°]	90	91.920
V [Å^3]	572.04	147.49
Z	4	1
D_{calc} [g/cm^3]	4.397	4.264
v [atoms]	56	14
I_G [bits/atom]	3.807	3.807
$I_{G,total}$ [bits/cell]	213.212	53.303

well. However, the role of structural complexity should not be neglected and one of the interesting problems that can be formulated is whether is it possible to use structural complexity measures to infer relative stability of different polymorphs?

Another interesting problem is whether structural complexity correlates with physical density of different polymorphs and how does it influence crystallization in natural systems. On the example of different copper oxysalt systems, we have recently demonstrated that structural complexity as another expression of configurational entropy does correlate with the ease of crystallization. For instance, in the Ostwald cascade of the $Cu_2(OH)_3Cl$ polymorphs (botallackite – atacamite – clinoatacamite), crystallization proceeds in the direction of increasing structural complexity, starting from simple (and less dense) botallackite and ending at most complex (and most dense) clinoatacamite (Krivovichev et al. 2017). In contrast, the $Cu_5(PO_4)_2(OH)_4$ polymorphs (pseudomalachite, ludjibaite and reichenbachite) do not differ essentially in their structural complexity, and this may explain their frequent simultaneous occurrence in nature and in synthesis experiments (Krivovichev et al. 2016b).

From this viewpoint, herein are considered two $Cu_3(AsO_4)(OH)_3$ polymorphs, clinoclase and gilmarite. In order to characterize fully their structural complexity, we report on the theoretical modeling of their hydrogen positions by means of the solid-state DFT method and use the obtained data to evaluate the hydrogen-bonding scheme and relative structural complexities of the two polymorphs.

Tab. 2 Atom coordinates for the crystal structure of clinoclase

Atom	x	y	z
As	0.3087	0.1499	0.1796
Cu1	0.7877	0.1400	0.3294
Cu2	0.8153	0.3813	0.1274
Cu3	0.3869	0.3531	0.4126
O1	0.4149	0.0710	0.0738
O2	0.8377	0.8423	0.3652
O3	0.1798	0.9469	0.2130
O4	0.4711	0.2205	0.2854
O5	0.7799	0.2034	0.4780
O6	0.8088	0.0943	0.1773
O7	0.1808	0.1670	0.4106
H1	0.7504	0.3491	0.4785
H2	0.9310	0.4708	0.6784
H3	0.1500	0.1668	0.4847

* coordinates of non-H atoms are from Eby and Hawthorne (1990); coordinates of H atoms are optimized using DFT method

2. Methods

2.1. Density functional theory (DFT) modeling

The CRYSTAL14 software package was employed for the solid-state DFT calculations (Dovesi et al. 2014). The Peintinger–Oliveira–Bredow split-valence triple-ζ (pob-TZVP) basis sets (Peintinger et al. 2013) were used for all atoms along with the hybrid Becke–3–Lee–Yang–Parr (B3LYP) functional, which provides excellent results for copper oxysalt crystals (Ruiz et al. 2006; Ruggiero et al. 2015; Krivovichev et al. 2016a, b). Geometry optimization was initiated with experimental determined crystal-structure models determined for clinoclase and gilmarite by Eby and Hawthorne (1990) and Sarp and Černý (1999), respectively (Tab. 1). The approximate positions of the H atoms have been proposed based on general crystal-chemical arguments. During the DFT optimization, all the non-H atom-positions and unit-cell parameters were kept constant, whereas the positions of the H atoms were allowed to relax. The unrestricted-spin calculation was used and the difference between α and β electrons was maintained for the first 10 cycles. The convergence criterion for the energy was set to 10^{-7} au. The optimized coordinates of the H atoms and the coordinates of the non-H atoms are given in Tabs 2 and 3 for clinoclase and gilmarite, respectively. Table 4 provides basic geometrical parameters of strong hydrogen bonds in both crystal structures.

2.2. Structural complexity calculations

In order to compare polymorphic variations in the system under study from the viewpoint of structural complexity, the latter was estimated as the Shannon information content per atom (I_G) and per unit cell ($I_{G,total}$). According to this approach developed by Krivovichev (2012, 2013), the complexity of a crystal structure can be quantitatively characterized by the amount of Shannon information it contains measured in bits (binary digits) per atom (bits/atom) and

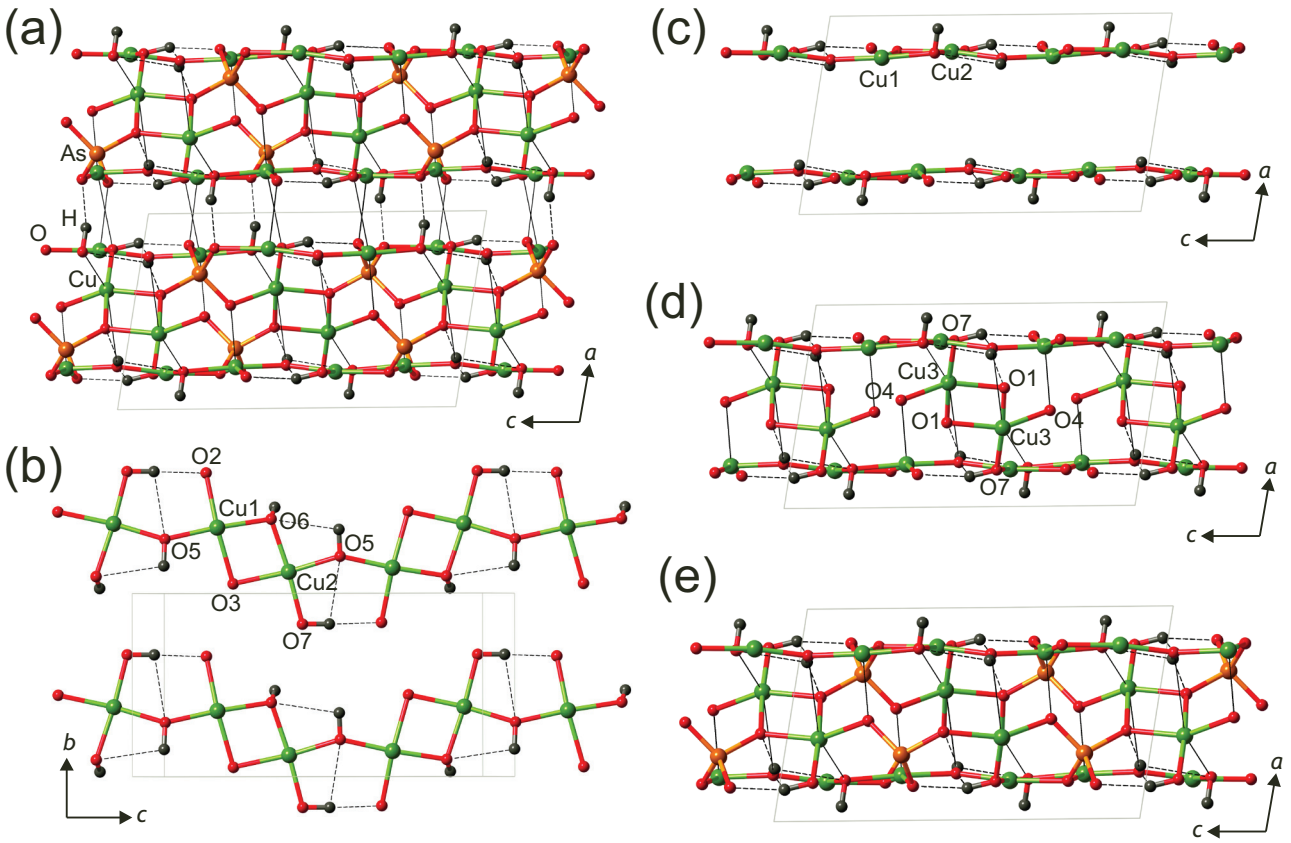

Fig. 1a – The crystal structure of clinoclase projected along the *b* axis. **b –** The sheet formed by $Cu1O_4$ and $Cu2O_4$ squares. **c –** Two adjacent sheets that belong to the same layer. **d –** Linkage of the two sheets by dimers of $Cu3O_6$ octahedra. **e –** The whole layer with inserted AsO_4 tetrahedra.

per unit cell (bits/cell), respectively. The concept of Shannon information, also known as Shannon entropy, used here originates from information theory and its application to various problems in graph theory, chemistry, biology, etc. The amount of Shannon information reflects diversity and relative proportion of individual objects, e.g., the number and relative proportion of different sites in an elementary unit-cell of a crystal structure. The calculation involves the use of the following equations:

$$I_G = -\sum_{i=1}^{k} p_i \log_2 p_i \quad \text{(bits/atom)} \qquad (1),$$

$$I_{G,total} = -v\, I_G = -v_i \sum_{i=1}^{k} p_i \log_2 p_i \quad \text{(bits/cell)} \qquad (2),$$

where k is the number of different crystallographic orbits (independent crystallographic Wyckoff sites) in the structure and p_i is the random-choice probability for an atom from the i^{th} crystallographic orbit, that is:

$$p_i = m_i / v \qquad (3),$$

where m_i is a multiplicity of a crystallographic orbit (i.e. the number of atoms of a specific Wyckoff site in the reduced unit-cell), and v is the total number of atoms in the reduced unit cell.

The information-based structural-complexity parameters for the $Cu_3(AsO_4)(OH)_3$ polymorphs were calculated using the TOPOS software package (Blatov et al. 2014) and are given in Tab. 1.

Tab. 3 Atom coordinates for the crystal structure of gilmarite

Atom	*x*	*y*	*z*
As	0.9987	0.0003	0.0001
Cu1	0.0492	0.6036	0.3224
Cu2	0.5489	0.3631	0.3568
Cu3	0.5723	0.8811	0.3869
O1	0.1620	0.2710	0.0710
O2	0.1880	0.8050	0.0740
O3	0.7030	0.5420	0.1540
O4	0.7430	0.0600	0.1860
O5	0.3710	0.6730	0.5380
O6	0.4830	0.2230	0.6300
O7	0.9050	0.8680	0.6530
H1	0.6544	0.4384	0.9465
H2	0.3467	0.7231	0.7446
H3	0.3306	0.2383	0.7264

* coordinates of non-H atoms are from Sarp and Černý (1999); coordinates of H atoms are optimized using DFT method

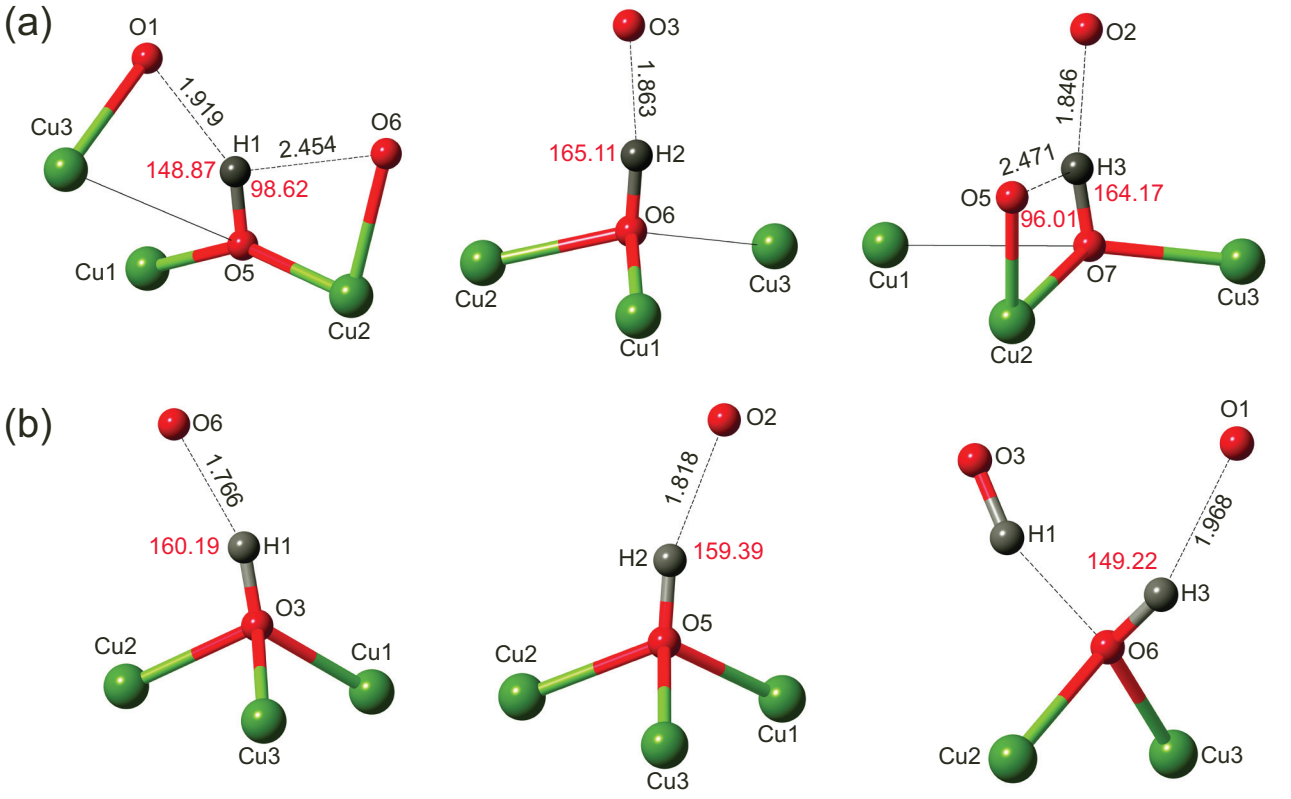

Fig. 2a – Coordination environments of hydroxyl groups in the crystal structure of clinoclase. **b** – Coordination environments of hydroxyl groups in the crystal structure of gilmarite.

3. Results

In the crystal structure of clinoclase, the Cu1 and Cu3 sites are in distorted [4+2] octahedral coordination (four short and two long Cu^{2+}–O bonds), whereas the Cu2 atom is coordinated by five O atoms to form a CuO_5 square [4+1] pyramid (four short and one elongated Cu^{2+}–O bonds; Ghose et al. 1965; Eby and Hawthorne 1990). The crystal structure is based upon two-dimensional layers parallel to (100) (Fig. 1a), which agrees well with the presence of perfect cleavage along this plane in clinoclase. The layers can be described as consisting of two sheets of the type shown in Fig. 1b. The $Cu1O_4$ and $Cu2O_4$ squares having short Cu^{2+}–O bonds share the O3···O_h6 edge to form dimers that are linked via O_h5 atom to form chains parallel to the *c* axis. Two adjacent sheets (Fig. 1c) are linked by dimers of edge-sharing $Cu3O_6$ octahedra (Fig. 1d). The $(AsO_4)^{3-}$ tetrahedra are located within the layer (Fig. 1e). The layers are linked via long Cu^{2+}–O bonds formed by the Cu1 and Cu2 atoms and via hydrogen bonds. The environments of the OH groups in clinoclase modeled by the DFT calculations are shown in Fig. 2a. There are three OH groups that form relatively strong two-center hydrogen bonds (see Tab. 4). The H···**A** bond lengths to the acceptor (**A**) O atoms are in the range of 1.846–1.919 Å, whereas the **D**–H···**A** angles (**D** = donor) vary from 148.87 to 165.11°. All acceptor O atoms belong to the arsenate groups. It is noteworthy that the OH5 and OH7 have additional close contacts (to O_h6 and O_h5 atoms, respectively), but it is unlikely that they correspond to meaningful hydrogen bonds. Both O6 and O5 atoms belong to hydroxyl groups, the H···O distances are longer than 2.45 Å, whereas the O–H···O angles are smaller than 98°.

The crystal structure of gilmarite is based on a three-dimensional framework consisting of layers of Cu polyhedra parallel to (001) and linked by (AsO_4) tetrahedra

Tab. 4 Geometrical parameters of hydrogen bonding system in the crystal structures of clinoclase and gilmarite

D–H	d(**D**–H) [Å]	d(H···**A**) [Å]	<**D**H**A** [°]	d(**D**···**A**) [Å]	**A**
Clinoclase					
O5–H1	0.965	1.912	148.87	2.783	O1
O6–H2	0.980	1.863	165.11	2.821	O3
O7–H3	0.979	1.846	164.17	2.801	O2
Gilmarite					
O3–H1	0.989	1.766	160.19	2.716	O6
O5–H2	0.986	1.818	159.39	2.762	O2
O6–H3	0.974	1.968	149.22	2.849	O1

* **D** = donor; **A** = acceptor

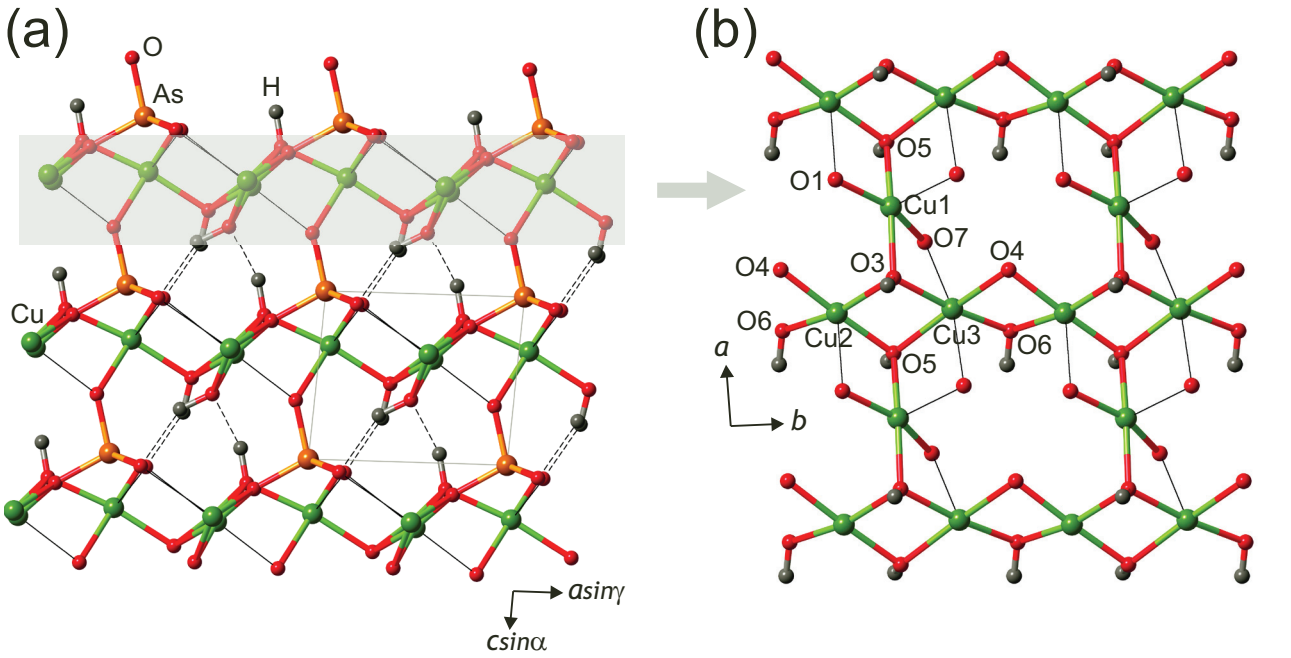

Fig. 3a – The crystal structure of gilmarite projected along the *b* axis. **b** – The layer of Cu polyhedra (highlighted by grey color in Fig. 3a).

(Fig. 3a). As in clinoclase, there are three independent Cu sites, of which Cu1 and Cu2 are [4+1]-coordinated to form CuO_5 square pyramids, whereas Cu3 has a distorted octahedral coordination. The structure of the Cu oxyhydroxy layer is shown in Fig. 3b. The $Cu2O_4$ and $Cu3O_4$ squares share edges to form infinite chains parallel to the *b* axis, and the chains are interlinked by the $Cu1O_4$ squares to form a two-dimensional layer. The layers are linked via (AsO_4) tetrahedra that have their triangular bases located in one layer and the fourth apex participating in the adjacent one. It is interesting that all tetrahedra have the same orientation, which results in a strongly non-centrosymmetric atomic arrangement (space group *P*1). The coordination environments of the OH groups are shown in Fig. 2b. As in clinoclase, three symmetrically independent OH groups are involved in relatively strong two-center hydrogen bonds with the H···**A** distances of 1.766–1.968 Å and the **D**–H···**A** angles of 149.22–160.19°. The most unusual feature of the hydrogen bonding in gilmarite is the presence of OH··· OH bond formed by the OH3–OH6 pair, where OH6 atom acts as both donor and acceptor of hydrogen bonding. As far as we know, this feature is rather uncommon in copper hydroxy-oxysalts. All the hydrogen bonds in gilmarite are located within the space between the Cu oxyhydroxy layers.

4. Discussion

The structural complexity parameters for clinoclase and gilmarite given in Tab. 1 indicate that, from the viewpoint of the information amount per unit cell, the structural arrangement of gilmarite is much simpler than that of clinoclase. According to the Goldsmith's simplexity principle (Goldsmith 1953) and its current interpretation (Krivovichev 2013, 2015), this may indicate that gilmarite is a metastable phase crystallized under some kinetically favored conditions. This suggestion is corroborated by the comparison of the values of physical density, which is equal to 4.264 g/cm^3 for gilmarite and 4.397 g/cm^3 for clinoclase. According to the Ostwald–Volmer rule (Holleman et al. 2001), for metastable crystallization, the less dense metastable phase forms first, due to the fact that, under supersaturation conditions, its nuclei reach their critical sizes faster than those of the stable phase (Fischer and Jansen 2002; Bach et al. 2013). The transformation from the metastable phase into a stable phase may occur along different routes that include: direct transformation (i.e. solid-state phase transition), solvent-mediated transformation (which includes dissolution of the metastable phase and precipitation of the stable one) and epitaxy-mediated transformation (when stable phase crystallizes on the surface of the metastable one) (Niekawa and Kitamura 2013). In the case under consideration, the direct gilmarite–clinoclase transformation must include phase transition of a reconstructive type, since the two structures are drastically different and may not be transformed one into another without breaking of the many chemical bonds. It is currently unclear which factors stabilize the formation of metastable gilmarite instead of stable clinoclase and understanding of these processes requires synthesis experiments.

5. Conclusions

In conclusion, we have used density functional theory (DFT) methods to model hydrogen bonding schemes in clinoclase and gilmarite. Whereas hydrogen bonds in clinoclase involve interactions between hydroxyl groups and O atoms of arsenate tetrahedra, the crystal structure of gilmarite features the OH···OH bonding, which is rather uncommon for copper hydroxy-oxysalts. Information-theory considerations of structural complexity of clinoclase and gilmarite show that the former is more complex than the latter, which indirectly indicates that gilmarite is a metastable phase. This suggestion is supported by the lower density of gilmarite compared to that of clinoclase.

Acknowledgements. I thank Juraj Majzlan and Frank Hawthorne for useful corrections on the first version of the manuscript. This work was supported by the Russian Science Foundation (grant 14-17-00071).

References

Bach A, Fischer D, Jansen M (2013) Metastable phase formation of indium monochloride from an amorphous feedstock. Z Anorg Allg Chem 639: 465–467

Blatov VA, Shevchenko AP, Proserpio DM (2014) Applied topological analysis of crystal structures with the program package ToposPro. Cryst Growth Des 14: 3576–3586

Bournon JL (1801) Sur le arséniates de cuvre, et de fer, du comté de Cornouailles. Jour des Mines 11: 35–62

Dovesi R, Orlando R, Erba A, Zicovich-Wilson CM, Civalleri B, Casassa S, Maschio L, Ferrabone M, De La Pierre M, D'Arco P, Noel Y, Causa M, Rerat M, Kirtman B (2014) CRYSTAL14: a program for *ab initio* investigation of crystalline solids. Int J Quantum Chem 114: 1287–1317

Eby RK, Hawthorne FC (1990) Clinoclase and the geometry of [5]-coordinate Cu^{2+} in minerals. Acta Crystallogr C46: 2291–2294

Fischer D, Jansen M (2002) Low-activation and solid-state syntheses by reducing transport lengths to atomic scales as demonstrated by case studies on $AgNO_3$ and AgO. J Amer Chem Soc 124: 3488–3489

Frost RL, Martens WN, Williams PA (2002) Raman spectroscopy of the phase-related basic copper arsenate minerals olivenite, cornwallite, cornubite and clinoclase. J Raman Spectrosc 33: 475–484

Ghose S, Fehlmann M, Sundaralingam M (1965) The crystal structure of clinoclase, $Cu_3AsO_4(OH)_3$. Acta Crystallogr 18: 777–787

Goldsmith JR (1953) A "simplexity principle" and its relation to "ease" of crystallization. J Geol 61: 439–451

Holleman AF, Wiberg F, Wiberg N (2001) Inorganic Chemistry. Academic Press, San Diego, CA, pp 1–507

Krivovichev SV (2012) Topological complexity of crystal structures: quantitative approach. Acta Crystallogr A68: 393–398

Krivovichev SV (2013) Structural complexity of minerals: information storage and processing in the mineral world. Mineral Mag 77: 275–326

Krivovichev SV (2015) Structural complexity of minerals and mineral parageneses: information and its evolution in the mineral world. In: Danisi R, Armbruster T (eds) Highlights in Mineralogical Crystallography. Walter de Gruyter, Berlin/Boston, pp 31–73

Krivovichev SV (2016) Structural complexity and configurational entropy of crystalline solids. Acta Crystallogr B72: 274–276

Krivovichev SV, Zolotarev AA, Pekov IV (2016a) Hydrogen bonding system in euchroite, $Cu_2(AsO_4)(OH)(H_2O)_3$: low-temperature crystal-structure refinement and solid-state density functional theory modeling. Mineral Petrol 110: 877–883

Krivovichev SV, Zolotarev AA, Popova VI (2016b) Hydrogen bonding and structural complexity in the $Cu_5(PO_4)_2(OH)_4$ polymorphs (pseudomalachite, ludjibaite, reichenbachite): combined experimental and theoretical study. Struct Chem 27: 1715–1723

Krivovichev SV, Hawthorne FC, Williams PA (2017) Structural complexity and crystallization: the Ostwald sequence of phases in the $Cu_2(OH)_3Cl$ system (botallackite–atacamite–clinoatacamite). Struct Chem 28:153–159

Lebernegg S, Tsirlin AA, Janson O, Rosner H (2013) Two energy scales of spin dimers in clinoclase $Cu_3(AsO_4)(OH)_3$. Phys Rev B87: 235117

Magalhães MCF, Pedrosa de Jesus JD, Williams PA (1988) The chemistry of formation of some secondary arsenate minerals of copper(II), zinc(II), and lead(II). Mineral Mag 52: 679–690

Majzlan J, Števko M, Dachs E, Benisek A, Plášil A, Sejkora J (2017) Thermodynamics, stability, crystal structure, and phase relations among euchroite, $Cu_2(AsO_4)(OH)\cdot 3H_2O$, and related minerals. Eur J Mineral, doi: 10.1127/ejm/2017/0029-2584

Martens WN, Frost RL, Kloprogge JT, Williams PA (2003) The basic copper arsenate minerals olivenite, cornubite, cornwallite, and clinoclase: An infrared emission and Raman spectroscopic study. Amer Miner 88: 501–508

Morse JW, Casey WH (1988) Ostwald processes and mineral paragenesis in sediments. Amer J Sci 288: 537–560

Niekawa N, Kitamura M (2013) Role of epitaxy-mediated transformation in Ostwald's step rule: a theoretical study. CrystEngComm 15: 6932–6941

Peintinger MF, Oliveira DV, Bredow T (2013) Consistent Gaussian basis sets of triple-zeta valence with polarization quality for solid-state calculations. J Comput Chem 34: 451–459

Pekov IV, Zubkova NV, Yapaskurt VO, Belakovskiy DI, Vigasina MF, Sidorov EG, Pushcharovsky DY (2015a) New arsenate minerals from the Arsenatnaya fumarole, Tolbachik Volcano, Kamchatka, Russia. III. Popovite, $Cu_5O_2(AsO_4)_2$. Mineral Mag 79: 133–143

Pekov IV, Zubkova NV, Belakovskiy DI, Yapaskurt VO, Vigasina MF, Sidorov EG, Pushcharovsky DY (2015b) New arsenate minerals from the Arsenatnaya fumarole, Tolbachik Volcano, Kamchatka, Russia. IV. Shchurovskyite, $K_2CaCu_6O_2(AsO_4)_4$ and dmisokolovite, $K_3Cu_5AlO_2(AsO_4)_4$. Mineral Mag 79: 1737–1753

Pekov IV, Zubkova NV, Yapaskurt VO, Polekhovsky YuS, Vigasina MF, Belakovskiy DI, Britvin SN, Sidorov EG, Pushcharovsky DY (2016) New arsenate minerals from the Arsenatnaya fumarole, Tolbachik Volcano, Kamchatka, Russia. VI. Melanarsite, $K_3Cu_7Fe^{3+}O_4(AsO_4)_4$. Mineral Mag 80: 855–867

Plášil J, Sejkora J, Škoda R, Novák M, Kasatkin AV, Škácha P, Veselovský F, Fejfarová K, Ondruš P (2014a) Hloušekite, $(Ni,Co)Cu_4(AsO_4)_2(AsO_3OH)_2(H_2O)_9$, a new member of the lindackerite supergroup from Jáchymov, Czech Republic. Mineral Mag 78: 1341–1353

Plášil J, Kasatkin AV, Škoda R, Škácha P (2014b) Klajite, $MnCu_4(AsO_4)_2(AsO_3OH)_2(H_2O)_{10}$, from Jáchymov (Czech Republic): the second world occurrence. Mineral Mag 78: 119–129

Ruggiero MT, Erba A, Orlando R, Korter TM (2015) Origins of contrasting copper coordination geometries in crystalline copper sulfate pentahydrate. Phys Chem Chem Phys 17: 31023–31029

Ruiz E, Llunell M, Cano J, Rabu P, Drillon M, Massobrio C (2006) Theoretical determination of multiple exchange couplings and magnetic susceptibility data in inorganic solids: the prototypical case of $Cu_2(OH)_3NO_3$. J Phys Chem B110: 115–118

Sarp H, Černý R (1999) Gilmarite, $Cu_3(AsO_4)(OH)_3$, a new mineral: its description and crystal structure. Eur J Mineral 11: 549–555